THE JOURNAL OF PHYSICAL CHEMISTRY Letters

Letter

pubs.acs.org/JPCL

Measurement of an Electronic Resonance in a Ground-State, Gas-Phase Acetophenone Cation via Strong-Field Mass Spectrometry

Timothy Bohinski, Katharine Moore Tibbetts, Maryam Tarazkar, Dmitri Romanov, Spiridoula Matsika, and Robert J. Levis*

Department of Chemistry, Department of Physics, and Center for Advanced Photonics Research, Temple University, Philadelphia, Pennsylvania 19122, United States

ABSTRACT: A one-photon ionic resonance is measured in the strong-field regime in acetophenone by recording the mass spectra as a function of excitation wavelength from 800 to 1500 nm. The ratio of the benzoyl to parent ion signals in the mass spectrum varies significantly with excitation wavelength, where the highest ratio observed upon excitation at 1370 nm (0.90 eV) indicates the presence of a one-photon resonance. At the resonant wavelength, the ratio of the benzoyl to parent ion signals increases linearly with laser intensity over a range from 1.1×10^{13} to 6.0×10^{13} W cm^{-2}. The ratio increases by a factor of 5 at 1370 nm with increasing pulse duration from 60 to 100 fs. Calculations using the equation of motion coupled cluster method support the existence of a one-photon transition from the ground ionic to a dissociative excited ionic state (0.87 eV), where motion of the acetyl group from a planar to nonplanar structure within the pulse duration enables the otherwise forbidden transition.

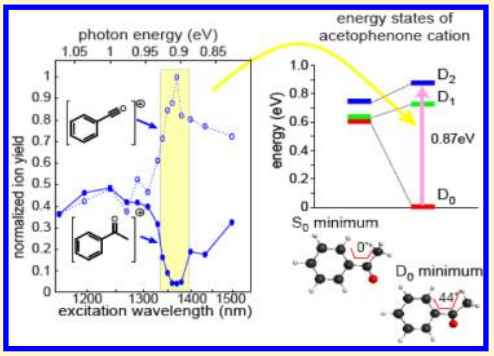

SECTION: Spectroscopy, Photochemistry, and Excited States

Spectroscopic detection of excited electronic states of the radical cation of a molecule is difficult, in part, due to the low number density of ground-state species that can be produced. Ionization methods such as electron impact[1] produce a plethora of initial states in the electronic manifold from which subsequent excitation can occur, and space charge effects limit the absolute number of ion states contained in a given volume. In addition, the calculation of excited ionic states is difficult given their typically open shell and multiconfigurational character.[2,3] This Letter presents a new method to measure the positions of low-lying excited ionic states using frequency-resolved, strong-field, near-infrared tunnel ionization and excitation. The method relies on tunnel ionization to selectively create ions in the ground state and on mass spectrometry to detect ion excitation to dissociative states with nearly unit probability.

Previous investigations[4] demonstrated that the fragmentation of polyatomic molecules was significantly suppressed using near-infrared (IR) wavelengths (1450 nm) for strong-field ionization (~10^{13} W cm^{-2}), as compared to the extensive fragmentation occurring when a strong-field 800 nm laser pulse excites the molecule. The lack of fragmentation after near-IR excitation suggests that less energy is deposited into excited electronic degrees of freedom, although the electronic state(s) of the parent molecular ions produced has not previously been assessed to our knowledge. Several studies suggest that resonances in the cationic state lead to enhanced fragmentation. It has been proposed that a resonance at 800 nm in the 1,4-cyclohexadiene cation results in enhanced fragmentation, whereas the production of only the parent ion in 1,3-cyclohexadiene was attributed to the lack of the cationic resonance at 800 nm.[5,6] An investigation of the ionization and fragmentation of naphthalene and anthracene revealed enhanced fragmentation at 800 nm in comparison with that at 1400 nm.[7] The fragmentation detected in both molecules at 800 nm was attributed to a resonance in the cationic states that is not excited at 1400 nm. However, another study attributes the fragmentation in naphthalene and anthracene at 800 nm to nonadiabatic excitation.[8] Cationic resonances have also been invoked to explain the strong-field fragmentation patterns for metal (Ni, Cr, Fe) carbonyl compounds.[9] In that investigation, analysis of photoelectron spectra revealed that $Ni(CO)_4^+$ has a resonance at 1350 nm, while $Fe(CO)_5^+$ has a resonance at 800 nm. The observed enhanced fragmentation of $Ni(CO)_4^+$ at 1350 nm and $Fe(CO)_5^+$ at 800 nm agrees with the hypothesis that a cationic resonance enhances molecular dissociation.[9] In related work, weak-field solution-phase transient absorption experiments have helped to elucidate the low-lying excited electronic structures in a plethora of molecules including carotenoids and Wurster's salts.[10,11]

Electronic resonances have been shown to be of central importance for interpreting coherent control measurements of fragmentation of halogenated methane molecules.[12−14] Time-resolved measurements using a strong-field 780 nm pump and a

Received: March 7, 2013
Accepted: April 22, 2013
Published: April 22, 2013

   dx.doi.org/10.1021/jz400516h | J. Phys. Chem. Lett. 2013, 4, 1587−1591

weak-field 780 nm probe revealed oscillations in the parent and fragment ion signals. The oscillations were attributed to wavepacket dynamics wherein fragmentation occurs whenever the ground-state ionic wavepacket encountered a one-photon resonance with an excited ionic dissociative state. The probability of population transfer of the wavepacket from the bound ionic state to the dissociative state was found to be linear in the intensity of the probe field. The dynamic response of the fragmentation channels demonstrated that it is possible to coherently control the dissociation of polyatomic systems.

Here, we measure the strong-field ionization mass spectra in acetophenone as a function of excitation wavelength in the IR. Acetophenone has been subjected to numerous experimental and theoretical investigations; in particular, calculations indicate the possibility for low-lying electronic states.[15] Photoelectron spectra of acetophenone report three low-lying excited states at 9.37, 9.55, and 9.77 eV. These are interpreted as states corresponding to the removal of an electron from the acetyl n orbital (forming the ionic ground state), the π orbital localized on the phenyl, and the delocalized π orbital that is caused by the interaction of the phenyl π orbital and the acetyl π orbital, respectively.[16,17] Here, we determine whether a one-photon resonance in the ground electronic state of the ion can be accessed in the excited-state manifold using a strong-field excitation pulse. Mass spectra are recorded as a function of laser wavelength, intensity, and pulse duration. The results are interpreted in the context of high-accuracy quantum calculations of the excited electronic states of the ion.

A regeneratively amplified Ti:sapphire laser produced 1 kHz, 1 mJ, 50 fs pulses centered at 790 nm. A 75/25 beam splitter redirects ~750 μJ of the output to a noncollinear optical parametric amplifier (nc-OPA) based upon the design of Wilson and Yakovlev.[18] The signal wavelength is readily tunable from 1150 to 1500 nm with pulse durations from 45 to 130 fs and is directed into the TOF-MS by a planoconvex lens, f = 20 cm. Attenuation of the beam is performed using a circular neutral density wheel.

Ion spectra were measured using a linear 1 m time-of-flight mass spectrometer operating in positive ion mode. A 500 μm slit was placed between the ionization and detection regions to restrict spatial averaging over the laser beam. A digital oscilloscope (LeCroy LT372) averaged 5000 spectra to produce the raw data. Acetophenone (Sigma-Aldrich) was leaked into the vacuum chamber by a controllable leak valve to attain a sample pressure of 3.5×10^{-6} Torr. A secondary leak valve controlled the amount of xenon that was allowed into the vacuum chamber to 7.5×10^{-6} Torr. The laser intensity at any wavelength and pulse energy was internally calibrated for each measurement with the ion signal produced by Xe. The Xe signals were fit to ADK calculations for tunnel ionization of a rare gas atom to determine the absolute laser intensity.[19] The background vacuum pressure in the chamber was ~1×10^{-8} Torr.

Electronic structure calculations were carried out using the Qchem[20] and Gaussian[21] series of programs. The geometry of the $C_6H_5COCH_3$ neutral molecule and the geometry of the radical cation were optimized at the B3LYP/6-31G(d) level of theory. The excited electronic states for the ion were calculated using the equation of motion, ionization potential, and coupled cluster singles and doubles (EOM-IP-CCSD) method[2] with the 6-311+G(d) basis set, while the oscillator strengths between D_0 and the higher ionic states were obtained using the excited-states EOM-CCSD approach (EOM-EE-CCSD) and the 6-31+G(d) basis set.

Mass spectra were measured for acetophenone as a function of excitation wavelengths ranging from 800 to 1500 nm and as a function of laser intensity ranging from 8×10^{12} to 8×10^{13} W cm^{-2}. The mass spectra contain the parent molecular ion (m/z = 120) or the benzoyl fragment ion (m/z = 105) as the largest feature in the mass spectrum, along with the smaller fragment ions including phenyl (m/z = 77), acetyl (m/z = 43), and methyl (m/z = 15) ions with decreasing signal yields, respectively. To show that we are accessing the tunneling regime in the region from 1150 to 1500 nm, we compared the fractional yield of ions with $m/z \leq 77$ (normalized to the total ion yield) as a function of laser intensity at six excitation wavelengths, shown in Figure 1. The fractional yield of small fragment ions is approximately twice as high at 800 nm as compared to that at the IR wavelengths, which suggests that multiphoton ionization is the dominant mechanism at 800 nm, while tunnel ionization dominates in the IR, in agreement with previous results.[4] The ground electronic state of the parent molecular ion is more likely to be populated in the tunnel ionization regime, allowing the enhanced production of "colder" ions in comparison with multiphoton excitation. Note that the methyl, acetyl, and phenyl radical cation yields are independent of the excitation wavelength. This strongly suggests that the internal energy of the tunnel ionization radical cation of acetophenone is independent of excitation wavelength from 1150 to 1500 nm. The ground radical cationic state can then serve as a launch state for spectroscopy in the strong field regime if a wavelength-tunable excitation source is used. Because there is no wavelength dependence for the ionization probability in the limit of tunnel ionization, the laser intensity can be accurately measured using the ion response for Xe leaked simultaneously into the chamber to calibrate the experimental intensity for each mass spectral measurement.[17]

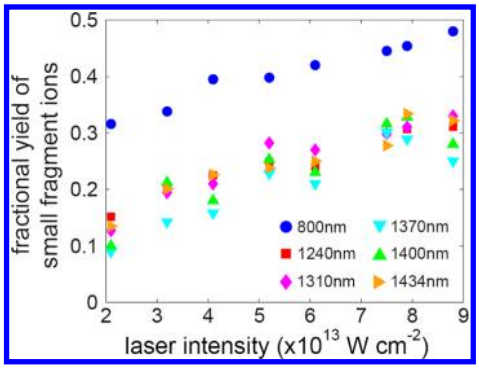

Figure 1. The fractional yield of small fragment ions, the sum of the integrated fragment signals at $m/z \leq 77$, as a function of laser intensity at excitation wavelengths ranging from 800 to 1434 nm.

At a fixed laser intensity, the acetophenone parent and benzoyl fragment ions exhibit an anticorrelation in their relative yields as a function of excitation wavelength from 1150 to 1500 nm. The integrated ion yields are plotted as a function of excitation wavelength in Figure 2 for laser intensities ranging from 2.1×10^{13} to 8.8×10^{13} W cm^{-2}. Each measurement is normalized to the maximum yield of the benzoyl ion at the highest laser intensity. At the shortest laser wavelengths, the two ion signals are not particularly sensitive to the wavelength (1150−1320 nm). However, at wavelengths longer than 1330

dx.doi.org/10.1021/jz400516h | J. Phys. Chem. Lett. 2013, 4, 1587−1591

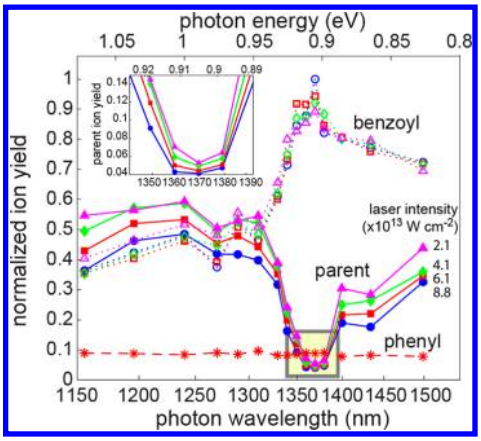

Figure 2. The integrated ion signal intensity for the phenyl, benzoyl, and parent ion at varying excitation wavelengths and intensities for acetophenone. The ion signals are normalized to the maximum benzoyl signal at the highest laser intensity. The dashed, solid, and dotted curves represent the phenyl, benzoyl, and parent ions, respectively, and color denotes the laser intensity. The phenyl ion signal is plotted at 6.1×10^{13} W cm^{-2}. The inset magnifies the region with depleted parent ion yields enclosed in the yellow box. Pulse durations were ~100 ± 10 fs throughout the tuning range.

nm, the signal of the benzoyl fragment ion increases and that of the parent decreases considerably. A maximum in the benzoyl fragment and a minimum in the parent ion are observed at the same wavelength, 1370 nm (a photon energy of ~0.9 eV). Further increase in the excitation wavelength results in a decline in the benzoyl fragment yield and an increase in the parent yield up to the reddest wavelengths available with our system. A similar response with respect to excitation wavelength was observed for the two ions for all laser intensities investigated. The response of the phenyl ion signal, also shown in Figure 2 (measured at a laser intensity of 6.1×10^{13}W cm^{-2}), reveals that lower mass fragments are not sensitive to this range of excitation wavelengths. A similar wavelength dependence was measured for all low mass ions for all intensities measured.

We propose that the wavelength-resolved strong-field response observed in Figure 2 arises from a one-photon transition from the ground electronic ion state to a low-lying dissociative state. To test the validity of the hypothesis that we are performing weak-field (linear) spectroscopy of ions using a strong-field laser pulse, we examine the signal response as a function of laser pulse duration and intensity. We can model the wavelength-dependent formation rate of the benzoyl fragment (B_λ) from the parent ion (A_λ) as a first-order unimolecular decay driven by the absorption of a photon by the following equation

$$\dot{B}_\lambda = \sigma_\lambda I(t) g(t) A_\lambda \quad (1)$$

where σ_λ is the cross section for excitation from the cationic ground state to the dissociative state as a function of wavelength, $I(t)$ is the envelope of the laser intensity, and $g(t)$ represents the time delay between ionization and excitation to the dissociative state. Integration of eq 1 over the pulse duration reveals that $B_\lambda \approx \sigma_\lambda I A_\lambda$, where I is the integrated intensity profile of the pulse. In the vicinity of the resonance, the parent ion is nearly depleted, as seen in the inset to Figure 2, for example, $A_{1370\ nm} \ll A_{1200\ nm}$. To normalize for the significantly reduced density of parent ion near the resonance, we divide eq 1 by A_λ and then plot B_λ/A_λ versus λ and I. The ratio B_λ/A_λ is plotted as a function of excitation wavelength for the 100 and 60 fs pulses at a laser intensity of 6.1×10^{13} W cm^{-2} in Figure 3. At both pulse durations, the ratio reaches a

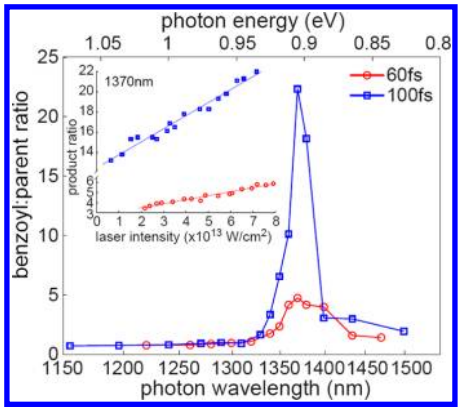

Figure 3. The benzoyl to parent ion ratio of the data taken from Figure 1 at 6.1×10^{13} W cm^{-2}. The red and blue curves are associated with data obtained with 60 and 100 fs pulses, respectively. The inset plots the normalized parent ion yield at the corresponding pulse durations obtained at the resonant excitation wavelength of 1370 nm.

maximum at ~0.9 eV. The integrated intensity of the feature produced from the 100 fs pulse is approximately 4 times more intense than that measured using the 60 fs pulse. Upon fitting to a Gaussian function, the full width at half-maximum (fwhm) of the ratio response for a 100 fs excitation pulse (blue squares) is approximately ~26 meV. The fwhm obtained from the raw benzoyl data in Figure 2 is ~50 meV. The latter resolution corresponds well with the ~30 meV spectral bandwidth of the laser pulse, retrieved from frequency-resolved optical gating measurements, convoluted with a 25 meV rovibrational distribution anticipated from the Boltzman distribution of the ground-state neutral at room temperature. The broader spectral bandwidth (~35 meV) of the 60 fs pulse produces a correspondingly broader fwhm of 40 meV in the ratio response function of Figure 3 and a fwhm of 70 meV based on the raw benzoyl data (not shown). This correspondence between the pulse spectral bandwidth and the resolution of the molecular response feature is consistent with a one-photon resonant process. If the molecular response arose from a higher-order excitation process, we would expect a narrower response function in comparison with the spectral bandwidth. Finally, the intensity of the excitation pulse does not shift the location of the resonance, as seen in Figure 2, suggesting that Stark shifting is not involved in the excitation process.

Additional evidence supporting the existence of a one-photon transition producing the observed wavelength-dependent response function comes from considering the molecular response as a function of laser intensity, as shown in the inset of Figure 3. At each intensity, the 100 fs pulse produces a higher product ratio in comparison with that for the 60 fs pulse. Both pulse durations reveal a linear response in the ratio function as a function of intensity at the resonant excitation wavelength of 1370 nm. The linear response with laser intensity is consistent with the intensity dependence given in eq 1 for a first-order excitation process.

Quantum chemistry calculations were performed to interpret the resonance feature and the pulse duration dependence of the benzoyl/parent ratio. Electronic structure calculations of the radical cation using the EOM-IP-CCSD/6-311+G(d) method

dx.doi.org/10.1021/jz400516h | J. Phys. Chem. Lett. 2013, 4, 1587−1591

show that the energy difference between the ground and first bright excited ionic states at the equilibrium geometry of the ion is 0.87 eV, which is in very good agreement with the measured resonance at 0.90 eV. The excited-state energy diagrams are summarized in Figure 4. The calculations show

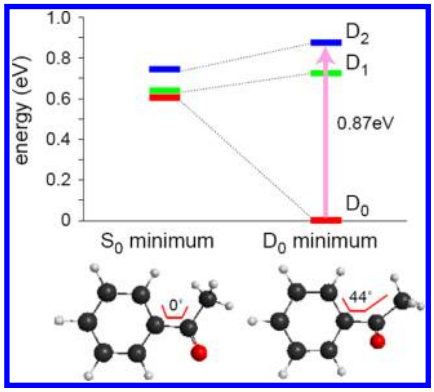

Figure 4. Energy-level diagram of the ground ionic and excited ionic states in acetophenone calculated at two geometries, the S_0 minimum (minimum of the neutral ground state) and the D_0 minimum (minimum of the ionic ground state). The zero of energy is set to the minimum energy of the cation ground state. Ground and excited states for the acetophenone ion were calculated at the EOMIP-CCSD/6-311+G(d) level of theory. Equilibrium geometries of the neutral and the cation are shown.

that the molecule, upon vertical ionization, is initially planar, and the spacing between the electronic states is very small; furthermore, selection rules dictate that transitions from the ground D_0 state to either the D_1 or D_2 state are forbidden. Once the molecule is ionized, the acetyl group initiates an out-of-plane torsional rotation with respect to the phenyl ring within the duration of the pulse. This torsional motion causes the gap between D_0 and the higher ionic states to increase and transforms the D_0 to D_2 transition from forbidden to allowed. The oscillator strengths for the transitions D_0 to D_1 and D_0 to D_2 are 0.002 and 0.046, respectively, at the minimum in the D_0 potential energy surface (see the cation equilibrium geometry in Figure 4). In the ground ionic state, the unpaired electron is on the phenyl ring, while in D_2, it is on the carbonyl group. Preliminary calculations indicate that as the C−CH_3 bond of the parent ion stretches leading to dissociation, the energy of D_0 increases, but the energy of D_2 decreases. The energy absorbed in the $D_0 \rightarrow D_2$ excitation presumably transforms to vibrational energy in the dissociative coordinate, leading to eventual formation of the benzoyl fragment ion. The dissociation energy has been calculated to be 0.82 eV[15]; thus, the photon energy deposited in D_2 is sufficient to lead to dissociation.

A larger ratio of benzoyl/parent ion is seen when the molecule is excited with a longer pulse duration. We attribute the increase in ratio to the acetyl group having additional time to rotate to the out-of-plane position, thus enhancing the transition dipole moment, inducing more excitation to the D_2 state with corresponding fragmentation. Thus, both the signal intensity and ultimate spectral resolution increase with increasing pulse duration. Further calculations on the dynamic transition dipole moment and the dissociation pathways will be highlighted in an upcoming paper.

An excited-state ionic resonance has been directly measured in the strong-field regime. The signature of the resonance is extracted from the near-infrared wavelength-dependent mass spectral response of the benzoyl fragment and parent ion signal after tunnel ionization. The resonance is consistent with a one-photon transition from a ground ionic state to an excited dissociative state. The yields of other fragment ion signals were independent of the excitation wavelength. The linear signal response of the benzoyl to parent ion ratio as a function of laser intensity, the response as a function of laser pulse duration/bandwidth, and the agreement with preliminary calculations support this hypothesis. The ratio of the benzoyl to parent signal can be manipulated by adjusting laser parameters including intensity, wavelength, and pulse duration.

AUTHOR INFORMATION

Corresponding Author

*E-mail: rjlevis@temple.edu.

Notes

The authors declare no competing financial interest.

ACKNOWLEDGMENTS

This work was supported by the National Science Foundation Grant Numbers CHE0957694 and CHE-1213614.

REFERENCES

(1) Becker, K. H.; Tarnovsky, V. Electron-Impact Ionization of Atoms, Molecules, Ions and Transient Species. *Plasma Sources Sci. Technol.* **1995**, *4*, 307.

(2) Krylov, A. I. Equation-of-Motion Coupled-Cluster Methods for Open-Shell and Electronically Excited Species: The Hitchhiker'S Guide to Fock Space. *Annual Review of Physical Chemistry*; Annual Reviews: Palo Alto, CA, 2008; Vol. *59*, pp 433−462.

(3) Matsika, S.; Krause, P. Nonadiabatic Events and Conical Intersections. In *Annual Review of Physical Chemistry*; Leone, S. R., Cremer, P. S., Groves, J. T., Johnson, M. A., Eds.; Annual Reviews: Palo Alto, CA, 2011; Vol. *62*, pp 621−643.

(4) Lezius, M.; Blanchet, V.; Ivanov, M. Y.; Stolow, A. Polyatomic Molecules in Strong Laser Fields: Nonadiabatic Multielectron Dynamics. *J. Chem. Phys.* **2002**, *117*, 1575−1588.

(5) Harada, H.; Shimizu, S.; Yatsuhashi, T.; Sakabe, S.; Izawa, Y.; Nakashima, N. A Key Factor in Parent and Fragment Ion Formation on Irradiation with an Intense Femtosecond Laser Pulse. *Chem. Phys. Lett.* **2001**, *342*, 563−570.

(6) Kotur, M.; Weinacht, T.; Pearson, B. J.; Matsika, S. Closed-Loop Learning Control of Isomerization Using Shaped Ultrafast Laser Pulses in the Deep Ultraviolet. *J. Chem. Phys.* **2009**, *130*, 134311.

(7) Yatsuhashi, T.; Nakashima, N. Effects of Polarization of 1.4 μm Femtosecond Laser Pulses on the Formation and Fragmentation of Naphthalene Molecular Ions Compared at the Same Effective Ionization Intensity. *J. Phys. Chem. A* **2005**, *109*, 9414−9418.

(8) Markevitch, A. N.; Nakashima, N.; Smith, S. M.; Romanov, D. A.; Schlegel, H. B.; Ivanov, M. Y.; Levis, R. J. Nonadiabatic Dynamics of Polyatomic Molecules and Ions in Strong Laser Fields. *Phys. Rev. A* **2003**, *68*, 011402.

(9) Trushin, S. A.; Fuss, W.; Schmid, W. E. Dissociative Ionization at High Laser Intensities: Importance of Resonances and Relaxation for Fragmentation. *J. Phys. B: At., Mol. Opt. Phys.* **2004**, *37*, 3987−4011.

(10) Amarie, S.; Arefe, K.; Starcke, J. H.; Dreuw, A.; Wachtveitl, J. Identification of an Additional Low-Lying Excited State of Carotenoid Radical Cations. *J. Phys. Chem. B* **2008**, *112*, 14011−14017.

(11) Grilj, J.; Buchgraber, P.; Vauthey, E. Excited-State Dynamics of Wurster's Salts. *J. Phys. Chem. A* **2012**, *116*, 7516−7522.

(12) Pearson, B. J.; Nichols, S. R.; Weinacht, T. Molecular Fragmentation Driven by Ultrafast Dynamic Ionic Resonances. *J. Chem. Phys.* **2007**, *127*, 131101.

(13) Nichols, S. R.; Weinacht, T. C.; Rozgonyi, T.; Pearson, B. J. Strong-Field Phase-Dependent Molecular Dissociation. *Phys. Rev. A* **2009**, *79*, 043407.
(14) Trallero, C.; Pearson, B. J.; Weinacht, T.; Gilliard, K.; Matsika, S. Interpreting Ultrafast Molecular Fragmentation Dynamics with Ab Initio Electronic Structure Calculations. *J. Chem. Phys.* **2008**, *128*, 124107.
(15) Anand, S.; Zamari, M. M.; Menkir, G.; Levis, R. J.; Schlegel, H. B. Fragmentation Pathways in a Series of CH_3CO_X Molecules in the Strong Field Regime. *J. Phys. Chem. A* **2004**, *108*, 3162−3165.
(16) Centineo, G.; Fragala, I.; Bruno, G.; Spampinato, S. Photoelectron Spectroscopy of Benzophenone, Acetophenone and Their Ortho-Alkyl Derivatives. *J. Mol. Struct.* **1978**, *44*, 203−210.
(17) Kobayashi, T.; Nagakura, S. Photoelectron Spectra of Substituted Benzenes. *Bull. Chem. Soc. Jpn.* **1974**, *47*, 2563−2572.
(18) Wilson, K.; Yakovlev, V. Ultrafast Rainbow: Tunable Ultrashort Pulses from a Solid-State Kilohertz System. *J. Opt. Soc. Am. B* **1997**, *14*, 444−448.
(19) Hankin, S. M.; Villeneuve, D. M.; Corkum, P. B.; Rayner, D. M. Intense-Field Laser Ionization Rates in Atoms and Molecules. *Phys. Rev. A* **2001**, *64*, 013405.
(20) Shao, Y.; Molnar, L. F.; Jung, Y.; Kussmann, J.; Ochsenfeld, C.; Brown, S. T.; Gilbert, A. T. B.; Slipchenko, L. V.; Levchenko, S. V.; O'Neill, D. P.; et al. Advances in Methods and Algorithms in a Modern Quantum Chemistry Program Package. *Phys. Chem. Chem. Phys.* **2006**, *8*, 3172−3191.
(21) Frisch, M. J.; Trucks, G. W.; Schlegel, H. B. et al. *GAUSSIAN 03*; Gaussian, Inc.: Pittsburgh, PA, 2003.